In Vitro Transport and Partitioning of AL-4940, Active Metabolite of Angiostatic Agent Anecortave Acetate, in Ocular Tissues of the Posterior Segment

Paul Missel,[1] James Chastain,[1] Ashim Mitra,[2] Uday Kompella,[3,4] Viral Kansara,[2] Sridhar Duvvuri,[2] Aniruddha Amrite,[3,5] and Narayan Cheruvu[3,6]

Abstract

Purpose. The purpose of this study was to evaluate partitioning into and transport across posterior segment tissues (sclera, retinal pigment epithelium (RPE)–choroid) of AL-4940, the active metabolite of angiostatic cortisene anecortave acetate (AL-3789).

Methods. Transport of [^{14}C]-AL-4940 was measured through RPE–choroid–sclera (RCS) and sclera, excised from Dutch Belted pigmented rabbits' eyes, in the directions of scleral to vitreal (S→V) and vitreal to scleral (V→S) for 3 h at 37°C using Ussing chambers. Tissue integrity was monitored by transepithelial electrical resistance (TEER), potential difference (PD), and biochemical assay (LDH). Partitioning in RPE–choroid and sclera was determined separately for both [^{14}C]-AL-4940 and [^{14}C]-AL-3789. Mathematical analysis for bilaminate membranes used partitioning and transport data to derive diffusion coefficients for 2 tissue layers sclera and RPE–choroid.

Results. Partitioning of drug in tissue was comparable for both [^{14}C]-AL-4940 and [^{14}C]-AL-3789. Partition coefficients of drug in tissue were 2.2 for sclera and about 4 for RPE–choroid. Permeability through sclera alone was about 3×10^{-5} cm/s and about 1×10^{-5} cm/s through the RCS tissue, irrespective of the direction of transport (S→V) or (V→S). Results from bioelectrical and biochemical evaluation of tissue with modified LDH assay provided evidence that the RCS tissue preparation remained viable during the period of transport study.

Conclusions. The thin RPE–choroid layer contributes significantly to resistance to drug transport, and diffusivity in this layer is 10 times less than in sclera. This experimental scheme is proposed as an important component for the development of a general ocular physiologically based pharmacokinetic model.

Introduction

Because of the growing incidence of ocular diseases in the aging population, interest has increased in developing pharmacotherapeutic treatment of diseases of the eye, particularly those affecting the posterior ocular segment.[1,2] Practical methods are being devised for treatment of the retina, choroid, and optic nerve by the sustained administration of drug through the exterior sclera. One such drug that was at one point being investigated for treatment of age-related macular degeneration was the cortisone molecule anecortave acetate. This agent was administered with a blunt-tipped, curved cannula, delivering a posterior juxtascleral depot: the hypothesis was that such a depot could provide a slow release of drug for diffusion across the posterior segment tissues into the macular portion of the retina.[3] Although attempts for developing a useful therapy were not successful, the studies conducted with this material nevertheless have utility as a model for understanding the fate of drugs administered in the posterior segment.

In the design of alternative ocular therapies, it is useful to obtain a general method for determining pharmacokinetic response to a variety of drug administration routes. We have

---

[1]Alcon Research, Ltd., Fort Worth, Texas.
[2]Division of Pharmaceutical Sciences, School of Pharmacy, University of Missouri-Kansas City, Missouri.
[3]Pharmaceutical Sciences, University of Nebraska Medical Center, Omaha, Nebraska.
[4]Current address: Pharmaceutical Sciences, University of Colorado, Denver, Colorado.
[5]Current address: Quintiles, Kansas City, Missouri.
[6]Current address: Covidien, St. Louis, Missouri.

attempted to develop general models capable of predicting pharmacokinetic response to intravitreal or posterior juxtascleral administration. Theoretical models used for mass transport through and elimination from the eye simultaneously accounted for both diffusivity and partitioning of drug into tissue,[4,5] and for influences of the choroidal sink and hydraulic flow.[6] Attempts were made to apply finite element analysis to simulate *in vivo* experiments, and to derive the tissue diffusion and partition coefficients from fits to experimental results.

Preliminary *in vivo* studies employed anecortave acetate, AL-3789, and its active metabolite, anecortave desacetate, AL-4940 (see Fig. 1). Anecortave acetate (4,9(11)-preganadien-17α,21-diol-3,20-dione-21-acetate, MW 386) is an angiostatic cortisene. Model experiments have presented this compound to the rabbit eye by 2 distinct modes of administration: intravitreal injection (Chastain and colleagues)[7] and insertion of a juxtascleral device.[5] The intravitreal injection experiment was designed in such a manner so as to facilitate the deduction of model system parameters, such as tissue-specific diffusion and partition coefficients and the choroidal elimination rate. It was anticipated that all of these parameters could be deduced from this single experiment by fitting to a finite element kinetic model.

This model would then be validated by the model's ability to predict the ocular drug distribution resulting from a completely different mode of drug administration, the juxtascleral device. However, the mathematical relationships amongst system parameters are extremely nonlinear and do not permit the unambiguous assignment of parameter values from a single *in vivo* experiment. Separate experiments are required to determine the diffusion and partition coefficients of drug in tissue. It is the purpose of this report to describe an appropriate method for making these separate independent determinations of these coefficients.

The posterior ocular tissue is a trilaminate structure comprised of neural retina, retinal pigment epithelium (RPE)–choroid, and sclera. Ideally one would characterize resistance to drug transport in each of these isolated tissues in separate experiments. However, it is impractical to isolate the choroid or retinal layers from the sclera or from each other to obtain a sample suitable for transport experiments. In addition, because the neural retina is easily damaged, inclusion of this portion of the retina, even in combined layers, is extremely difficult. Only the sclera can be reliably isolated and its transport properties examined directly independently of the influence of the other layers. The transport properties can dependably be examined only by measuring the influence of RPE–choroid on transport through the sclera.
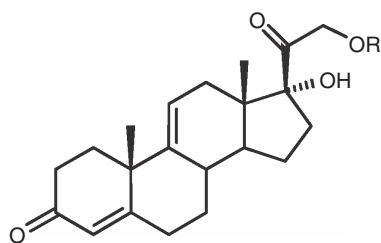
FIG. 1. Structure of anecortave acetate (AL-3789, R = acetate) or the corresponding desacetate (AL-4940, R = hydrogen).

Previous experiments demonstrated that transport of dexamethasone sodium *m*-sulfobenzoate (DMSB),[8] gancyclovir,[9] mannitol,[10,11] and folic acid[11] through intact retinal pigment epithelium–choroid–sclera (RCS) membrane is reduced several fold compared with transport through sclera alone, indicating that the RPE–choroid layer contributes most of the resistance to transport for these molecules. Some authors determined both drug diffusion coefficients and partition coefficients directly from the transport data, using the time-lag[12] method. This method typically requires reliable data at frequent time intervals early in the transport experiment.

Mathematical methods are available[13] for the analysis of multilaminate membranes, and were adapted using the data available[8,9] to estimate how rugged the determination of partition and diffusion coefficients might be from lag-time data alone. In applying the lag-time method for bilaminate membranes to these test datasets, it was found that a high degree of uncertainty exists in the determinations of either diffusion or partition coefficients (Missel, P.J., 2000, unpublished results).

Thus we examined the transport of radiolabeled drug through both excised intact RCS membrane and through sclera alone, which had been denuded of RPE–choroid. Rather than relying upon the lag-time method to measure the partition coefficient, a separate set of *in vitro* experiments was undertaken to directly measure the partition coefficient of drug between buffer and each posterior ocular tissue type. There are literature reported methods for estimating eye tissue partition coefficients.[10,14] In this way, we demonstrate methods for unambiguously determining the diffusion and partition coefficients in posterior ocular tissues.

In the 1950s, Ussing and Zerahn introduced a diffusion cell model for ion transport studies across frog skin that was combined with a voltage clamp technique.[15] This technique has been adapted and improved for investigations in other tissues. The *in vitro* Ussing chamber system mounts animal mucosal membrane between 2 side-by-side diffusion cells. It has been used to evaluate the absorption characteristics of new drugs at the membrane level.[16–20] Continuous validation of the integrity and the viability of the tissue is assessed by measuring electrophysiological parameters.[15,20] The Ussing chamber system is a convenient *in vitro* model for assessing barrier properties of posterior segment tissues and for investigating factors influencing drug permeability.

Methods

Reagents and solutions

[^{14}C]-AL-3789 and [^{14}C]-AL-4940 were obtained from Amersham Biosciences. Cremophor® EL was obtained from Sigma.

Other reagents were of analytical grade, and were used as received. Distilled, deionized water was used in the preparation of all buffers and mobile phases.

Dulbecco's phosphate buffer solutions (DPBS) for transport experiments contained 129 mM NaCl, 2.5 mM KCl, 7.4 mM Na_2HPO_4, 1.3 mM KH_2PO_4, 1 mM $CaCl_2$, 0.74 mM $MgSO_4$, 5 mM glucose, and 0.01% vol/vol cremophore. Immediately before transport experiments began, a fresh solution of the [^{14}C]-AL-4940 was prepared in dimethyl sulfoxide (DMSO) and spiked into the buffer solution to yield a

drug concentration of 0.1764 μmol/mL. Final concentration of DMSO in the buffer was not >0.5% wt/vol.

Animals

Dutch Belted pigmented rabbits weighing 2–2.5 kg were employed in these studies. All the procedures performed on the animals were conformed to the ARVO Resolution for the Use of Animals in Ophthalmic and Vision Research. Prior to harvesting tissues, rabbits were anesthetized using ketamine HCl (35 mg/kg) and xylazine (5 mg/kg) administered intramuscularly, and then euthanized by an overdose of sodium pentobarbital administered through the marginal ear vein. Eyes were excised immediately after euthanasia and the posterior segment was carefully removed after cutting along the corneal–scleral limbus junction.

Ussing chamber setup

The Ussing chamber apparatus (USS4S, World Precision Instruments, Inc., Sarasota, FL) that was employed for performing transport experiments was the same as used previously (schematic diagram appears in Fig. 1 of Ref. [11]). In brief, the tissue is mounted between 2 fluid cells, which are maintained at equal hydrostatic pressure to avoid tissue damage. Fluid circulation is achieved by injecting compressed air at a controlled rate into tubing that connects each cell with reservoirs mounted 20–25 cm above each cell. Fluid temperature was thermostated at 37°C.

Tissue preparation for transport studies

The posterior segment, RCS, was placed with the scleral side down in a Petri dish containing DPBS at 37°C and washed to remove any blood and extraneous matter present. A small circular shaped tissue section was dissected carefully with the aid of microscissors and mounted on the Ussing chamber. In case of scleral tissue preparation, neural retina, RPE, and choroid were carefully peeled off from sclera with forceps prior to tissue mounting.

Transport experiments

All transport experiments were carried out in quadruplicate. Transport experiments were performed across sclera and RCS from sclera to vitreous (S→V) and vitreous to sclera (V→S) directions at 37°C for 3 h. Five milliliters of DPBS was added to donor and receiver chambers and the tissue was allowed to equilibrate for 30 min. At time 0, 1 mL of drug solution was added to the donor side and 1 mL of buffer solution to the receiver side, and compressed air was applied to effect stirring. Samples (200 μL) were withdrawn from the receiver chamber at predetermined time intervals. Five milliliters of scintillation cocktail was added to the samples and analyzed using a Beckman scintillation counter (Beckman Instruments Inc., Fullerton, CA; Model LS-6500). Flux values for [14C]-AL-4940 were calculated by dividing the slope, obtained by plotting a cumulative amount of the compound permeated vs. time, with the area available for diffusion, that is, 0.1256 cm^2. The permeability values were calculated by dividing the flux values by the concentration of permeant in the donor as shown in equation 1.

$$P_T = (V/A \times 1/C_0) \times (dC/dt) \qquad (1)$$

Here P_T = apparent permeability coefficient (cm/s), the subscript T denoting the tissue type (T = S for sclera, RCS for intact RCS membrane), V = volume of the receiver chamber (cm^3), A = tissue surface area (cm^2), C_0 = donor concentration at start of experiment, and dC/dt = change in the concentration of compound in receiver chamber over time (min). Statistical tests were performed to compare the permeability values. Student's t-test was employed at 95% confidence level to test the differences between permeability values.

Electrophysiological measurements

Electrophysiological studies were performed with RCS tissue preparation during the transport experiments to monitor tissue viability. Transepithelial electrical resistance (TEER) and potential difference (PD) were recorded at predetermined times during experiments with calomel electrodes attached to 3% agar gel bridges and EVOM voltmeter. The electrodes were allowed to equilibrate with buffer at 37°C before insertion into the donor and receiver chambers.

LDH assay

Viability of the tissues was assessed by a modified lactate dehydrogenase (LDH) assay. Tissue (RCS) was mounted on the Ussing chamber and incubated under same experimental conditions as described for transport studies. Tissue damage was assessed by measuring LDH activity released in the medium, expressed as a percentage of total tissue LDH activity. LDH released into the buffer during incubations was normalized to a percentage of the total tissue LDH content. Tissue specimens upon removal from the eyes were frozen by immersion in liquid nitrogen and rapidly thawed. These tissues were homogenized using tissue homogenizer and served as a reference. LDH efflux assay and protein content of the tissues were determined according to directions of assay kit with slight modifications.

Partitioning studies

All experiments were conducted in triplicate. The posterior segment tissues were dissected and isolated into neural retina, RPE–choroid and sclera. These tissues were placed immediately upon dissection into preweighed microcentrifuge tubes. The average weights of the sclera, RPE–choroid and retina were 0.195 ± 0.027, 0.026 ± 0.010, and 0.014 ± 0.007 g, respectively. One milliliter of phosphate-buffered saline (PBS) was added and the tubes were incubated at 37°C for 30 min. Tubes were then spiked with either 0.0156 μCi [14C]-AL-3789 or 0.0175 μCi [14C]-AL-4940, vortexed, and incubated for an additional 6 or 12 h.

The tubes were then centrifuged at 5,000 rpm for 5 min and the supernatants were collected in preweighed scintillation vials and the vials were reweighed. One milliliter of PBS was added to the tissue pellets and the tubes were vortexed and centrifuged at 5,000 rpm for 5 min. The wash was collected in preweighed scintillation vials and reweighed. The tissue pellets were removed with forceps and transferred to preweighed scintillation vials and reweighed. The tissues were solubilized using 1 mL Solvable® overnight at 50°C. Scintillation vials containing supernatants, tissue pellets, and tissue washes were spiked with 12.5 mL of scintillation

cocktail, the vial surfaces were cleaned, and the [^{14}C] activity was counted using a liquid scintillation counter.

The partition coefficient values were calculated after normalizing the radioactivity to tissue weights. Total mass balance of radioactivity distributed between tissue, supernatant, and wash was accounted for within 20%. Control DPBS solutions spiked in the same way as tissue samples produced scintillation counts to within 5% of the amounts expected. In all cases the amount of radioactivity in the wash was found to be negligible.

Mathematical methods

Although in principle an attempt to characterize the transport properties of retina, choroid, and sclera as 3 separate layers in a trilaminate membrane may be possible, it is experimentally impractical and mathematically tedious to attempt. Thus we consider the simplified case of a bilaminate membrane, in which the RPE and choroid comprise a single layer (layer RC), and the sclera comprises layer S. Figure 2 illustrates the steady-state drug concentration distribution in a hypothetical bilaminate tissue assembly installed between donor and receptor compartments at a particular time during a transport experiment. To derive the diffusion coefficients in each layer of the bilaminate membrane, the partition coefficient of drug in each layer must first have been determined, and 2 different transport experiments must be conducted. The first of these is to measure the rate of drug transport through sclera alone that has been denuded of the RPE–choroid. From this we may obtain an estimate of the diffusion coefficient in this layer as follows:

$$D_S = \frac{P_S h_S}{k_S} \tag{2}$$
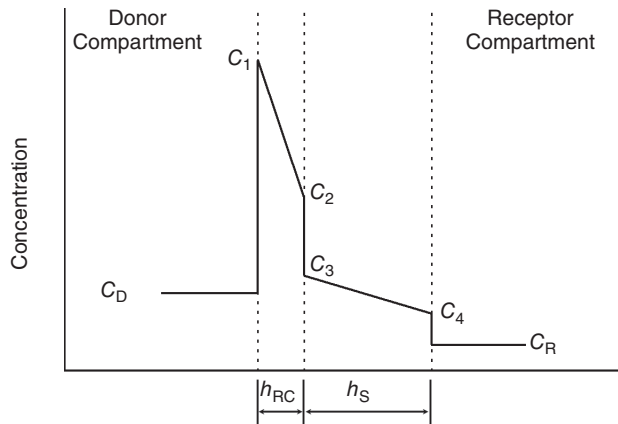
FIG. 2. Hypothetical steady-state drug concentration distribution in a bilaminate membrane during a transport experiment, illustrating the effect of partitioning. Abbreviations: C_D, donor concentration; C_R, concentration in receptor compartment; C_1, concentration just inside the first bilaminate layer in contact with the donor compartment; C_4, concentration just inside the second layer in contact with the receptor compartment; C_2, concentration just inside the first layer in contact with the second layer; C_3, concentration just inside the second layer in contact with the first layer. h_{RC} and h_S are the thicknesses of the RPE–choroid and sclera, respectively.

where D_S is the diffusion coefficient (cm^2/s), P_S is the permeability as determined from the transport experiment (cm/s), h_S is the thickness of the sclera (cm), and k_S is the partition coefficient of drug in sclera. In the second experiment, the transport is measured through the intact bilaminate membrane. The diffusivities and thicknesses of both layers contribute to the resistance to drug transport, so a mathematical approach is required to deduce the value of D_{RC}, the diffusion coefficient in the RPE–choroid, treated as a single layer. We use an approach based upon the series partitioning model of the cornea described by Lang and Stiemke.[21] The fluxes through layers 1 and 2 are given by:

$$J_{RC} = \frac{D_{RC}(C_1 - C_2)}{h_{RC}} \tag{3}$$

$$J_S = \frac{D_S(C_3 - C_4)}{h_S} \tag{4}$$

At steady state, $J_{RC} = J_S$. We also make use of the following relations:

$$C_1 = k_{RC}C_D \tag{5}$$

$$C_3 = \frac{k_S}{k_{RC}}C_2 \tag{6}$$

$$C_4 = k_S C_R \tag{7}$$

where C_D is the concentration in the donor solution, C_R is the concentration in the receptor solution, and k_{RC} is the average partition coefficient of the RPE–choroid layer. Substituting eqs. (5–7) into the equality $J_{RC} = J_S$, using eqs. (3) and (4), we obtain:

$$\frac{D_{RC}(k_{RC}C_D - C_2)}{h_{RC}} = \frac{D_S\left(\dfrac{k_S}{k_{RC}}C_2 - k_S C_R\right)}{h_S}. \tag{8}$$

Solving eq. (8) for C_2, we obtain:

$$C_2 = \frac{C_R D_S h_{RC} k_{RC} k_S + C_D D_{RC} h_S k_{RC}{}^2}{D_S h_{RC} k_S + D_{RC} h_S k_{RC}} \xrightarrow{\mathrm{Lim}\,C_R \to 0} \frac{C_D D_{RC} h_S k_{RC}{}^2}{D_S h_{RC} k_S + D_{RC} h_S k_{RC}} \tag{9}$$

where we have evaluated the expression in the limit of zero receptor concentration, which will greatly simplify the mathematics below. At steady state, the flux through either one of the layers is simply P_{RCS} times the donor concentration, where P_{RCS} is the permeability measured through the intact bilaminate membrane. We evaluate the right hand side of eq. (8) in the limit $C_R \to 0$ and set equal to the measured flux:

$$J_S = D_S \frac{\left(\dfrac{k_S}{k_{RC}}\right)C_2}{h_S} = P_{RCS}C_D \tag{10}$$

Substituting eq. (9) for C_2 into eq. (10), we obtain:

$$\left[\frac{D_S k_S}{h_S k_{RC}}\right]\left[\frac{C_D D_{RC} h_S k_{RC}{}^2}{D_S h_{RC} k_S + D_{RC} h_S k_{RC}}\right] = P_{RCS}C_D \tag{11}$$

Solving this expression for D_S, we obtain:

$$D_{RC} = \frac{D_S k_S h_{RC} P_{RCS}}{k_{RC}[D_S k_S - h_S P_{RCS}]} \tag{12}$$

The correctness of this result may be proved by recasting it in the form of series resistance to transport for a bilaminate membrane. Rearranging Eq. (12) slightly, we obtain:

$$\frac{D_{RC}k_{RC}}{h_{RC}} = \frac{D_S k_S P_{RCS}}{[D_S k_S - h_S P_{RCS}]} = \frac{P_{RCS}}{1 - \frac{h_S}{D_S k_S}P_{RCS}} \quad (13)$$

From Eq. (2) we infer:

$$P_S = \frac{D_S k_S}{h_S} \quad (14)$$

Similarly,

$$P_{RC} = \frac{D_{RC}k_{RC}}{h_{RC}} \quad (15)$$

Thus Eq. (13) can be rewritten as follows:

$$P_{RC} = \frac{P_{RCS}}{1 - \frac{P_{RCS}}{P_S}} \quad (16)$$

Taking the inverse of both sides, we obtain:

$$\frac{1}{P_{RC}} = \frac{1}{P_{RCS}} - \frac{1}{P_S} \quad (17)$$

Rearranging, we obtain the mathematical statement that the resistance to transport of the bilaminate membrane is the sum of the resistances of each of the layers, as transport resistance is inversely proportional to the permeability[10]:

$$\frac{1}{P_{RCS}} = \frac{1}{P_{RC}} + \frac{1}{P_S} \quad (18)$$

Results

Transport of [14C]-AL-4940 across RCS and sclera

Transport of [14C]-AL-4940 across RCS and sclera, in the vitreal to scleral direction and vice versa is shown in Figure 3. Permeability values for [14C]-AL-4940 are summarized in
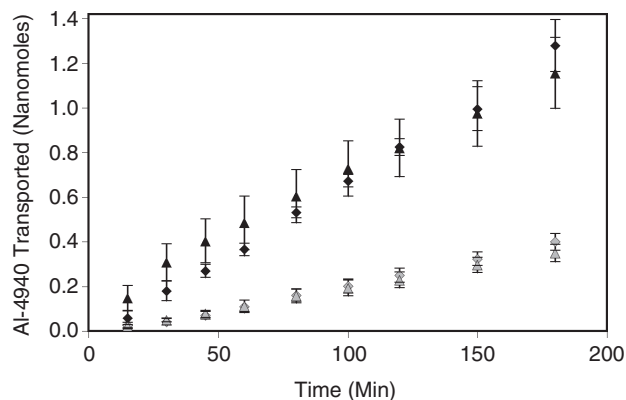
FIG. 3. Transport of [14C]-AL-4940 across sclera and retinal pigment epithelium–choroid–sclera (RCS) membrane. Solid symbols: transport across sclera. Shaded symbols: transport across RCS membrane. Triangles: donor compartment adjacent to vitreous side. Diamonds: donor compartment against outer sclera. Each measurement represents mean ± SD of 4 separate determinations.

Table 1. No significant differences among polarized fluxes of [14C]-AL-4940 were observed across the sclera or RCS in the S→V and V→S directions. However, significant differences in the flux values of [14C]-AL-4940 were observed across sclera and RCS in both directions. As shown in Table 2, permeability of [14C]-AL-4940 across sclera was nearly 3-fold higher as compared with RCS in both S→V and V→S directions.

Electrophysiological measurements

The TEER values across RCS were 86.40 and 85.14 Ohm/cm² in DPBS and DPBS with 0.5% DMSO wt/vol, respectively. The transepithelial PD values across RCS were 2.91 and 3.05 mV in DPBS and in DPBS with 0.5% DMSO wt/vol, respectively. Steady-state values for TEER and PD for RCS remained relatively constant during the 3-h study period and 4 h after removal, indicating that the viability of the RCS was maintained over the experimental period (Fig. 4A and 4B). A major advantage of electrophysiological measurements was that damaged tissues can be recognized and replaced before addition of the test compound and the viability of the membranes can be continuously monitored. In contrast, studies where permeability markers were used in the absence of electrophysiological measurements, information about membrane damage was not available until the completion of analysis.

Biochemical evaluation of the tissue

The biochemical activity of the RCS was investigated by a modified LDH assay. Tissue specimens mounted on the Ussing chamber simulated transport experiments and specimens incubated upon removal from the rabbit eye served as reference. Percentage viability of RCS was found to be 94% and 91% in the DPBS and DPBS with 0.5% DMSO wt/vol, respectively. Results from the LDH assay confirmed that 3 h of incubation in the Ussing chamber did not appear to have any major influence on the viability and integrity of the tissues (Fig. 5).

Partitioning of [14C]-AL-3789 and [14C]-AL-4940 in posterior ocular tissues

Results for both compounds appear in Table 2. Partitioning at 12 h is ranked RPE–choroid > retina ≥ sclera for each compound. The degree of partitioning appears to approach equilibrium after 12 h. There is not much difference between partitioning values in the various tissues between the 2 drug species. Since we are treating the RCS as a bilaminate, and not a trilaminate membrane, we can only attribute a single

TABLE 1. [14C]-AL-4940 PERMEABILITY VALUES ACROSS RCS AND SCLERA TISSUE PREPARATION

Tissue	Direction	Permeability (cm/s) × 10⁻⁵
RPE–choroid–sclera (RCS)	Sclera to vitreal side	1.05 (± 0.08)*
	Vitreal to scleral side	0.91 (± 0.10)**
Sclera	Sclera to vitreal side	3.27 (± 0.34)
	Vitreal to scleral side	2.63 (± 0.30)

*Statistical difference between RCS (S→V) and sclera (S→V) at a level of $P < 0.05$.

**Statistical difference between RCS (V→S) and sclera (V→S) at a level of $P < 0.05$.

TABLE 2. PARTITIONING OF [^{14}C]-AL-3789 AND [^{14}C]-AL-4940 IN RABBIT SCLERA,
CHOROID–RPE, AND RETINA

| | Partition coefficient[a] | | | |
| | [^{14}C]-AL-3789 | | [^{14}C]-AL-4940 | |
Tissue	6 h	12 h	6 h	12 h
Sclera	1.62 ± 0.19	2.12 ± 0.12	1.86 ± 0.25	2.19 ± 0.13
Choroid–RPE	6.94 ± 3.69	5.17 ± 1.33	3.42 ± 2.23	4.94 ± 1.95
Retina	0.52 ± 0.11	2.91 ± 1.15	0.39 ± 0.25	2.17 ± 0.62

[a]The partition coefficients are calculated as a ratio of concentration in the tissue (μCi/g)
and concentration in the supernatant (μCi/g).

partition coefficient to the single RPE–choroid layer. A good rough assignment that strikes a reasonable balance between the values measured for the RPE–choroid and retina is 4. We select a value of 2.2 for the sclera. In the case of AL-4940, the partition coefficient was similar in sclera (2.2) and retina (2.3), but ~2-fold higher in RPE–choroid (5.0). Only the sclera and RPE–choroid values were used in transport calculations.

Determination of tissue diffusion coefficients

We must select reasonable values for the thicknesses of the sclera and RPE–choroid layers. Amongst various domestic animals, the sclera varies in thickness[22] from about 0.02 to 0.08 cm. We selected a value of 0.03 cm, which matches values measured from similar tissue samples from adult rabbits in separate studies (Missel, unpublished data, 2000). A value of 0.011 cm for an average thickness of the retina is supported by histology[23,24] and optical coherence tomography measurements[24] in adult rabbits. The thickness of the choroid is problematic because of its collapse to one-half or less its *in vivo* thickness postmortem due to the lack of perfusion.[25] Assessment of thickness by histology can be misleading because of the variability in thickness caused by partial collapse of vessels. We estimate the choroidal thickness to be 0.007 cm based upon the weights of numerous dissections from circular punches of posterior segment tissues from adult rabbits.[7] Thus the total combined thickness of retina and choroid is assumed to be 0.018 cm. If only the single layer of the RPE (thickness 14 μm)[26] is included with the choroid, the combined thickness is reduced to 0.0084 cm.

From Table 1, the values of the permeabilities measured in either direction are quite comparable, and we select $P_S \approx 3.0 \times 10^{-5}$ cm/s and $P_{RCS} \approx 1.0 \times 10^{-5}$ cm/s. From eq. (2), the value obtained for D_S is:

$$D_S = \frac{P_S h_S}{k_S} = \frac{(3 \times 10^{-5}\,\text{cm/s})(0.03\,\text{cm})}{2.2} = 4.1 \times 10^{-7}\,\text{cm}^2/\text{s}$$

which is about an order of magnitude lower than the diffusivity of the drug in water or vitreous fluid. Using this value for D_S in eq. (12), we obtain an estimate for D_{RC}:

$$D_{RC} = \frac{D_S k_S h_{RC} P_{RCS}}{k_{RC}[D_S k_S - h_S P_{RCS}]}$$

$$= \frac{(4.1 \times 10^{-7}\,\text{cm}^2/\text{s})(2.2)(.018\,\text{cm})(1 \times 10^{-5}\,\text{cm/s})}{(4)\left[(4.1 \times 10^{-7}\,\text{cm}^2/\text{s})(2.2) - (0.03\,\text{cm})(1 \times 10^{-5}\,\text{cm/s})\right]}$$

$$= 6.74 \times 10^{-8}\,\text{cm}^2/\text{s}$$

If the smaller thickness for the RC layer is used, including only the choroid and the RPE layer, the value for D_{RC} is reduced to 3.15×10^{-8} cm^2/s.

Discussion

The horizontal Ussing chamber has been used as an *in vitro* model to study the transepithelial transport properties of mammalian RPE or choroid preparations in various species (cow, pig, dog, cat, monkey, rabbit).[10,16,27–29] Frambach
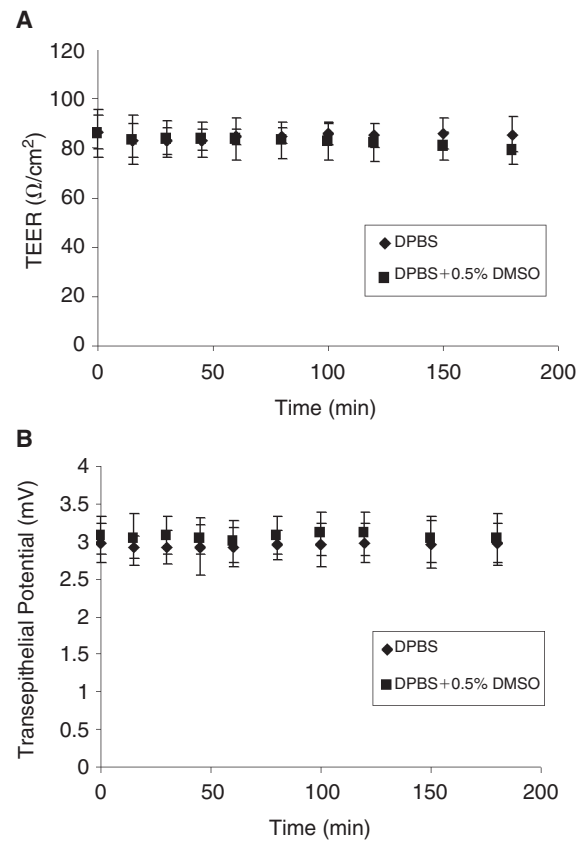
FIG. 4. (**A**) Transepithelial electrical resistance (TEER) values for retinal pigment epithelium–choroid–sclera (RCS) for 3 h at 37°C in Dulbecco's phosphate buffer solutions (DPBS; pH 7.4). (**B**) Transepithelial potential values for RCS for 3 h at 37°C in DPBS (pH 7.4) measured using EVOM voltmeter. Each data point represents the mean ± SD of 4 separate determinations.
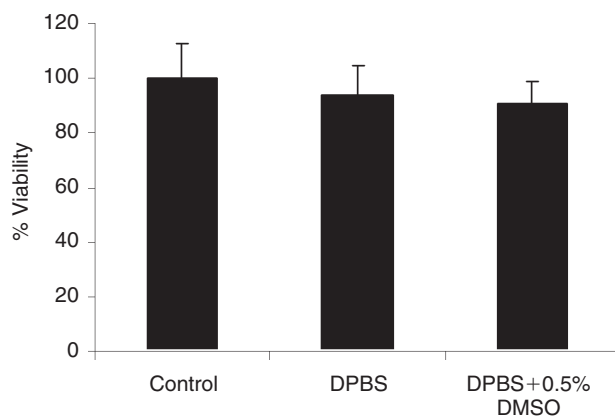
FIG. 5. Tissue viability study for retinal pigment epithelium–choroid–sclera (RCS) for 3 h at 37°C in Dulbecco's phosphate buffer solutions (DPBS; pH 7.4) with 0.5% dimethyl sulfoxide (DMSO; vol/vol) using lactate dehydrogenase (LDH) assay. Controls are fresh tissues assumed to be 100% viable. The total LDH quantified in the lysates of freshly isolated tissue formed a basis to assess the relative viability of tissue with the other 2 treatments. For the 2 treatments, tissue was exposed to the respective treatments for 3 h and the LDH released into the medium was quantified. Each data point represents the mean ± SD of 4 separate determinations.

et al.[30] were the first to report transport studies through RCS preparations from rabbit. The fragile nature of the RPE–choroid in the rabbit would make it extremely difficult if not impractical to study this thin layer by itself. Therefore, we performed permeability of AL-4940 across intact RCS because it maintains the tissue in a viable state by the continuous supply of compressed air—a situation that is closer to the *in vivo* situation than when circulation is effected only by mechanical means.[31] Further, we assessed the permeability across sclera alone in order to estimate the permeability of RPE–choroid. The lack of a significant difference in the rate of drug transport between the vitreous to sclera and sclera to vitreous directions in RCS or sclera suggests the absence of significant active transport under the conditions of the study. Therefore, the distribution in ocular tissue was explained and modeled simply on the basis of its physicochemical diffusion and partitioning properties.

During permeability studies across RCS membrane, the integrity of the tissue was continuously monitored using TEER and PD. A decrease in the TEER during the course of the experiment would indicate potential loss of the integrity of RPE tight junctions. The PD reflects the ability of RPE to maintain active ion transport.[32] Resistance values were comparable with those previously reported for RCS preparations in the rabbit,[30] whereas the transepithelial PD that averaged 2.94 mV was lower than recorded previously.[30] However, since no significant differences in either TEER or (PD)) were observed during the entire experiment, it was determined that tissue integrity was not altered during the transport experiments (Fig. 4A and 4B).

Tissue viability was further confirmed by measuring LDH, a cytosolic enzyme released only when there is cell damage.[33,34] The color intensity of a red formazan product resulting from the conversion of a tetrazolium salt (INT) in a

30-min coupled enzymatic assay quantitates the amount of LDH released.[35,36] The high percentage viability established by the LDH assay results in Figure 5 provides further evidence that the tissue was viable throughout the period of transport measurements.

The combination of biochemical assay (LDH assay) and electrophysiological measurements (TEER and PD) indicated that the tissue remains viable during the entire transport study period. Since PD and TEER remained stable, the equivalent short-circuit current (I_{eq} = PD/TEER) also remained constant, indicating that the solutes assessed did not affect the active ion transport across the tissue.

Chemical substances will partition into the various ocular tissues corresponding to their lipophilicity. This general fact can be advantageous for optimizing delivery of topically applied compounds, without requiring detailed measurements of partitioning into selected tissues.[37] Physiologically based pharmacokinetic (PBPK) modeling attempts to make more quantitative predictions of chemical species distribution, and have undertaken the systematic direct measurement of partition coefficients in each of the tissues of interest.[38,39] Rather than attempting to deduce the tissue partition coefficient from a lag-time coefficient, as has been done in other ocular PBPK studies,[8,9,40] we undertook the direct measurement of partitioning in the separate tissues of the posterior segment. This removed the ambiguity in the determination of the partition coefficient, and also eliminated the strong mathematically nonlinear interaction between the assignment of partition and diffusion coefficients from a single experimental dataset. In this study, we observed that the partitioning of AL-3789 and AL-4940 in the various posterior segment tissues is comparable after 12 h of equilibration. Since AL-3789 is rapidly converted to AL-4940 in ocular tissue, we anticipate that the permeability and partition coefficients of AL-4940 would be useful in predicting its delivery following administration of AL-3789. The inclusion of the acetate group increases the lipophilicity of AL-3789 relative to AL-4940. This increased lipophilicity may have led to a more rapid equilibration of AL-3789 with choroid–RPE, compared with AL-4940 (see Table 2). One ambiguity in the scintillation counting measurements is the possibility that the chemical species, particularly AL-3789, may have undergone conversion by metabolism in part, which is a limitation of this technique.

The value measured for drug permeability through sclera, 3×10^{-5} cm/s compares favorably with the values found for a variety of small drug molecules that range from about 1 to 5×10^{-5} cm/s.[41] Although Figure 2 is not drawn to scale with respect to the proportion of tissue and cell volumes, the relative proportion of RPE–choroid to sclera is correct, as are the magnitudes of the concentration discontinuities at the tissue interfaces as calculated by equation (9). The resistance to drug transport in each layer is inversely proportional to the slope of the change in concentration with distance in each of the 2 tissue layers. The majority of the resistance to transport in the intact RCS membrane rests in the RPE–choroid layer, contributing about two-third of the resistance. This is somewhat comparable with the situation observed by Pitkänen and colleagues[42] for a hydrophobic substance. They found the RPE to be a major barrier for the transport of hydrophilic substances, but for lipophilic materials the RPE–choroid and sclera were approximately equivalent barriers. Kansara and Mitra found that RPE–choroid offered no additional

resistance to transport across intact RCS as compared with sclera alone for the lipophilic drug diazepam.[11]

It must be kept in mind that these measurements are, in a sense, static descriptions of the tissue, since one of the very important features that is operational *in vivo* that cannot be reproduced in these *in vitro* models is the effect of the vascular choroidal clearance. The magnitude of the choroidal clearance rate must be deduced from *in vivo* measurements, simulated from a geometrically accurate model of the eye to which the materials property determinations from these *in vitro* measurements have been appropriately assigned to the various anatomical regions. In our future models of specific *in vivo* experiments, we will make these material property assignments and use the value of the choroidal clearance strength as a single adjustable parameter to provide the best fit to the time dependence of drug clearance after bolus intravitreal injection. Other type of dynamic barriers can also be included.[43] Another important limitation to keep in mind is the fact that animal species differences and pigmentation will impact tissue partitioning and transport.[44]

One alternative source for retinal tissue is to use *in vitro* cell culture systems. The *in vitro* techniques for evaluating retinal drug delivery mainly involve primary cultures of retinal cells and human retinal pigment epithelial cell line, ARPE-19. Applications of such *in vitro* techniques can be informative and relatively inexpensive; however, current *in vitro* systems suffer from significant limitations. For instance, the ARPE-19 cell line is leaky in nature due to the relatively low density of tight junctions between epithelial cells, contrary to physiological conditions, and hence not entirely representative of *in vivo* conditions. Also, retinal cell culture models often do not faithfully reconstitute many of the differentiated properties of the cell from which they are derived.[45] Moreover, the interaction between RPE and underlying neural retina is absent in the cell culture models.[46] Excised tissues, as employed in this study, are expected to retain the RPE architecture similar to the *in vivo* models.

Conclusion

Based on the partition coefficient and permeability estimates obtained in this study for AL-4940, we anticipate that its *in vivo* delivery can be adequately explained and modeled. The mathematical method proposed for determining transport through separate layers is more mathematically robust than deductions based upon lag-time data. The analysis requires the independent measurement of tissue partition coefficients for the various layers in advance of the mathematical treatment. Although a similar method could conceivably be adapted for experiments in tri- and higher-order laminate membranes, it is unlikely that the data would be of sufficient quality to support the fitting of such data. It would be better in such cases to make separate experiments for combinations of bilaminate structures if they could be practically obtained.

Acknowledgment/Disclosure

References

1. Geroski, D.H., and Edelhauser, H.F. Transscleral drug delivery for posterior segment disease. *Adv. Drug Deliv. Rev.* 52:37–48, 2001.
2. Feng, X., Pilon, K., Yaacobi, Y., et al. Extraocular muscle insertions relative to the fovea and optic nerve: humans and rhesus macaque. *Invest. Ophthalmol. Vis. Sci.* 46:3493–3496, 2005.
3. D'Amico, D.J., Goldberg, M.F., Hudson, H., et al.; Anecortave Acetate Clinical Study Group. Anecortave acetate as monotherapy for treatment of subfoveal neovascularization in age-related macular degeneration: twelve-month clinical outcomes. *Ophthalmology.* 110:2372–83; discussion 2384, 2003.
4. Missel, P.J. Finite element modeling of diffusion and partitioning in biological systems: the infinite composite medium problem. *Ann. Biomed. Eng.* 28:1307–1317, 2000.
5. Missel, P., Stevens, L., Chastain, J., et al. A clear vision for drug delivery. *Fluent News* 15:s8–s10, 2006.
6. Missel, P.J. Hydraulic flow and vascular clearance influences on intravitreal drug delivery. *Pharm. Res.* 19:1636–1647, 2002.
7. Chastain, J.E., Missel, P.J., Kiehlbauch, C.C., and Dahlin, D.C. *Ocular Pharmacokinetics of Radioactivity in Rabbits Following Intravitreal Administration of 3H-Anecortave Acetate*, AAPS meeting, Toronto, November 2002, AAPS PharmSci. 4(S1):332, 2002.
8. Ohtori, A., and Tojo, K. *In vivo/in vitro* correlation of intravitreal delivery of drugs with the help of computer simulation. *Biol. Pharm. Bull.* 17:283–290, 1994.
9. Tojo, K., Nakagawa, K., Morita, Y., et al. A pharmacokinetic model of intravitreal delivery of ganciclovir. *Eur. J. Pharm. Biopharm.* 47:99–104, 1999.
10. Cheruvu, N.P., and Kompella, U.B. Bovine and porcine transscleral solute transport: influence of lipophilicity and the Choroid-Bruch's layer. *Invest. Ophthalmol. Vis. Sci.* 47:4513–4522, 2006.
11. Kansara, V., and Mitra, A.K. Evaluation of an *ex vivo* model implication for carrier-mediated retinal drug delivery. *Curr. Eye Res.* 31:415–426, 2006.
12. Crank, J. *The Mathematics of Diffusion*. 2nd ed. Oxford: Oxford University Press; 1975; p. 51.
13. Barrer, R.M. Diffusion and permeation in heterogeneous media. In: Crank, J., Park, G.S., eds. *Diffusion in Polymers*. New York: Academic Press; 1968; p. 176.
14. Kadam, R.S., and Kompella, U.B. Influence of lipophilicity on drug partitioning into sclera, choroid–rpe, retina, trabecular meshwork, and optic nerve. *J. Pharmacol. Exp. Ther.* 332:1107–1120, 2009.
15. Ussing, H.H., and Zerahn, K. Active transport of sodium as the source of electric current in the short-circuited isolated frog skin. *Acta Physiol. Scand.* 23:110–127, 1951.
16. Tsuboi, S. Measurement of the volume flow and hydraulic conductivity across the isolated dog retinal pigment epithelium. *Invest. Ophthalmol. Vis. Sci.* 28:1776–1782, 1987.
17. Sinko, P.J., Lee, Y.H., Makhey, V., et al. Biopharmaceutical approaches for developing and assessing oral peptide delivery strategies and systems: *in vitro* permeability and *in vivo* oral absorption of salmon calcitonin (sCT). *Pharm. Res.* 16:527–533, 1999.
18. Pantzar, N., Lundin, S., Wester, L., et al. Bidirectional small-intestinal permeability in the rat to some common marker molecules *in vitro*. *Scand. J. Gastroenterol.* 29:703–709, 1994.
19. Ohtake, K., Maeno, T., Ueda, H., et al. Poly-L-arginine predominantly increases the paracellular permeability of hydrophilic macromolecules across rabbit nasal epithelium *in vitro*. *Pharm. Res.* 20:153–160, 2003.
20. Polentarutti, B.I., Peterson, A.L., Sjöberg, A.K., et al. Evaluation of viability of excised rat intestinal segments in the Ussing chamber: investigation of morphology, electrical parameters, and permeability characteristics. *Pharm. Res.* 16:446–454, 1999.
21. Lang, J.C., and Stiemke, M.M. Biological barriers to ocular delivery. In: Reddy, I.W., ed. *Ocular Therapeutics and Drug Delivery: A Multidisciplinary Approach*. Lancaster: Technomic; 1996; pp. 51–132.

22. Prince, J.H., Eglitis, I., and Ruskell, G.L. *Anatomy and Histology of the Eye and Orbit in Domestic Animals.* Springfield, IL: CC Thomas; 1960; pp. 267–274.

23. Reichenbach, A., Schnitzer, J., Friedrich, A., et al. Development of the rabbit retina. I. Size of eye and retina, and postnatal cell proliferation. *Anat. Embryol.* 183:287–297, 1991.

24. Ge, J., Luo, R., and Guo, Y. Corrective change of retinal thickness measured by optical coherence tomography and histologic studies. *Yan Ke Xue Bao.* 15:153–5, 178, 1999.

25. Coleman, D.J., Silverman, R.H., Chabi, A., et al. High-resolution ultrasonic imaging of the posterior segment. *Ophthalmology.* 111:1344–1351, 2004.

26. Bron, A.J., Tripathi, R.C., and Tripathi, B.J. *Wolff's Anatomy of the Eye and Orbit.* 8th ed. New York: Oxford University Press; 1997; p. 461.

27. Steinberg, R.H., Miller, S.S., and Stern, W.H. Initial observations on the isolated retinal pigment epithelium-choroid of the cat. *Invest. Ophthalmol. Vis. Sci.* 17:675–678, 1978.

28. Tsuboi, S., and Pederson, J.E. Volume flow across the isolated retinal pigment epithelium of cynomolgus monkey eyes. *Invest. Ophthalmol. Vis. Sci.* 29:1652–1655, 1988.

29. Kimura, M., Araie, M., and Koyano, S. Movement of carboxy-fluorescein across retinal pigment epithelium-choroid. *Exp. Eye Res.* 63:51–56, 1996.

30. Frambach, D.A., Valentine, J.L., and Weiter, J.J. Initial observations of rabbit retinal pigment epithelium-choroid-sclera preparations. *Invest. Ophthalmol. Vis. Sci.* 29:814–817, 1988.

31. Lennernäs, H., Nylander, S., and Ungell, A.L. Jejunal permeability: a comparison between the ussing chamber technique and the single-pass perfusion in humans. *Pharm. Res.* 14:667–671, 1997.

32. Artursson, P., Ungell, A.L., and Löfroth, J.E. Selective paracellular permeability in two models of intestinal absorption: cultured monolayers of human intestinal epithelial cells and rat intestinal segments. *Pharm. Res.* 10:1123–1129, 1993.

33. Legrand, C., Bour, J.M., Jacob, C., et al. Lactate dehydrogenase (LDH) activity of the cultured eukaryotic cells as marker of the number of dead cells in the medium [corrected]. *J. Biotechnol.* 25:231–243, 1992.

34. Korzeniewski, C., and Callewaert, D.M. An enzyme-release assay for natural cytotoxicity. *J. Immunol. Methods.* 64:313–320, 1983.

35. Goergen, J.L., Marc, A., and Engasser, J.M. Determination of cell lysis and death kinetics in continuous hybridoma cultures from the measurement of lactate dehydrogenase release. *Cytotechnology.* 11:189–195, 1993.

36. Allen, M., Millett, P., Dawes, E., et al. Lactate dehydrogenase activity as a rapid and sensitive test for the quantification of cell numbers *in vitro. Clin. Mater.* 16:189–194, 1994.

37. Higashiyama, M., Inada, K., Ohtori, A., et al. Improvement of the ocular bioavailability of timolol by sorbic acid. *Int. J. Pharm.* 272:91–98, 2004.

38. Andersen, M.E., Sarangapani, R., Reitz, R.H., et al. Physiological modeling reveals novel pharmacokinetic behavior for inhaled octamethylcyclotetrasiloxane in rats. *Toxicol. Sci.* 60:214–231, 2001.

39. Emond, C., Birnbaum, L.S., and DeVito, M.J. Use of a physiologically based pharmacokinetic model for rats to study the influence of body fat mass and induction of CYP1A2 on the pharmacokinetics of TCDD. *Environ. Health Perspect.* 114:1394–1400, 2006.

40. Tojo, K. A pharmacokinetic model for ocular drug delivery. *Chem. Pharm. Bull.* 52:1290–1294, 2004.

41. Prausnitz, M.R., and Noonan, J.S. Permeability of cornea, sclera, and conjunctiva: a literature analysis for drug delivery to the eye. *J. Pharm. Sci.* 87:1479–1488, 1998.

42. Pitkänen, L., Ranta, V.P., Moilanen, H., et al. Permeability of retinal pigment epithelium: effects of permeant molecular weight and lipophilicity. *Invest. Ophthalmol. Vis. Sci.* 46:641–646, 2005.

43. Kim, S.H., Lutz, R.J., Wang, N.S., et al. Transport barriers in transscleral drug delivery for retinal diseases. *Ophthalmic Res.* 39:244–254, 2007.

44. Cheruvu, N.P., Amrite, A.C., and Kompella, U.B. Effect of eye pigmentation on transscleral drug delivery. *Invest. Ophthalmol. Vis. Sci.* 49:333–341, 2008.

45. Siegel, G.M. The golden age of retinal cell culture. *Mol. Vis.* 5:4, 1999.

46. Marmorstein, A.D., Peachey, N.S., and Csaky, K.G. *In vivo* gene transfer as a means to study the physiology and morphogenesis of the retinal pigment epithelium in the rat. *Methods.* 30:277–285, 2003.

Address correspondence to:
Dr. Paul J. Missel
Alcon Research, Ltd.
Drug Delivery
R2-45
6201 South Freeway
Fort Worth, TX 76134

E-mail: paul.missel@alconlabs.com